

# Magnetic anisotropy of critical current in nanowire Josephson junction with spin-orbit interaction

T. YOKOYAMA<sup>1,2</sup> and YU. V. NAZAROV<sup>1</sup>

<sup>1</sup> *Kavli Institute of Nanoscience, Delft University of Technology, Lorentzweg 1, 2628 CJ, Delft, The Netherlands*

<sup>2</sup> *Center for Emergent Matter Science, RIKEN institute, 2-1 Hirosawa, Wako, Saitama 351-0198, Japan*

PACS 74.45.+c – Proximity effects; Andreev reflection; SN and SNS junctions

PACS 75.70.Tj – Spin-orbit effects

PACS 73.63.-b – Electronic transport in nanoscale materials and structures

**Abstract** – We develop and study theoretically a minimal model of semiconductor nanowire Josephson junction that incorporates Zeeman and spin-orbit effects. The DC Josephson current is evaluated from the phase-dependent energies of Andreev levels. Upon changing the magnetic field applied, the critical current oscillates manifesting cusps that signal the  $0-\pi$  transition. Without spin-orbit interaction, the oscillations and positions of cusps are regular and do not depend on the direction of magnetic field. In the presence of spin-orbit interaction, the magnetic field dependence of the current becomes anisotropic and irregular. We investigate this dependence in detail and show that it may be used to characterize the strength and direction of spin-orbit interaction in experiments with nanowires.

**Introduction.** – Semiconductor nanowire is an attractive nanostructure to investigate spin physics arising from the spin-orbit (SO) interaction. A strong SO interaction and the manipulation of electron spin in InAs and InSb nanowires have been reported [1,2]. Such nanowires are candidates to realize the topological physics. It has been suggested that the superconductor-nanowire junction forms the Majorana fermion at edge of superconducting region [3]. The zero-bias anomaly of conductance, which is attributed to the Majorana bound states, has been measured in the transport experiments for InSb nanowire recently [4–6]. The nanowire Josephson junctions have been also examined beyond topologically non-trivial regime [7–13].

The Josephson effect is one of the most fundamental phenomena in superconductivity. The spin degree of freedom enriches physics of the Josephson effect, e.g., causing the  $0-\pi$  transition in ferromagnetic Josephson junction [14]. In recent studies, the parity conservation of quasiparticles was shown to cause the  $4\pi$ -periodicity of current-phase relation [15] and increase of critical current [16]. The effect of SO interaction on the Josephson effect also has been studied. The SO interaction in combination with magnetic field shifts the current-phase relation, which results in the anomalous Josephson current that persists even at zero phase difference [17–19]. In previous studies, we have attributed the anomalous effect to the spin-dependent channel mixing in the nanowire [18, 19].

In this letter, we study the magnetic field dependence of critical current in the presence of SO interaction. We develop

a minimal model that encompasses the effect. The critical current oscillation accompanying the  $0-\pi$  transition has been demonstrated in ferromagnetic Josephson junctions [14]. Recent experiment has reported a similar oscillation in the magnetic field in InSb nanowire [13]. The oscillation should be affected by the effective SO field. The SO interaction has been discussed as the origin of anisotropies of level anticrossing, g-factor etc [1, 2, 20]. We investigate the anisotropy of critical current magnetic field dependence. The distance between the cusps of critical current is modulated by the angle between magnetic and effective SO field. If the SO interaction is strong, the two cusps are closer to each other. From the measurement of the anisotropy of critical current [13], the direction of the effective SO field can be determined. We also discuss the parity effect on the critical current oscillation.

**Model.** – Let us formulate a minimal model. We consider an one-dimensional semiconductor nanowire connected to two superconductors, as shown in Fig. 1(a), that supports a single transport mode. The nanowire has no impurities and is infinitely long along the  $x$  axis. Therefore, the electron and hole propagations are completely ballistic. The spin singlet superconducting pair potential  $\Delta(x)$  is induced in the nanowire by the proximity effect.

The Bogoliubov-de Gennes (BdG) equation reads as [21]

$$\begin{pmatrix} H - E_F & \Delta(x) \\ \Delta^*(x) & -(\mathcal{T}H\mathcal{T}^{-1} - E_F) \end{pmatrix} \begin{pmatrix} \psi_e \\ \phi_h \end{pmatrix} = E \begin{pmatrix} \psi_e \\ \phi_h \end{pmatrix}. \quad (1)$$

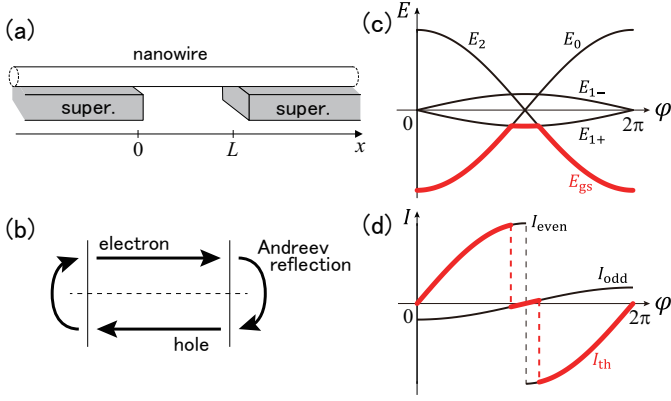


Fig. 1: Minimal model of a semiconductor nanowire Josephson junction. (a) Schematic view of the model. The nanowire is infinitely long along the  $x$  axis. The electron and hole transport in the ballistic nanowire. The pair potential is induced in the nanowire at  $x < 0$  and  $x > L$  by the proximity effect. (b) Schematic view of Andreev bound state formed by right-going electron and left-going hole. (c) Energies of junction without quasiparticles and with one or two quasiparticles as functions of phase difference  $\varphi$ . The two middle curves correspond to one quasiparticle states, the levels of which are split by a weak magnetic field. Red thick curve corresponds to the ground state. (d) Josephson currents in even and odd parity states at zero temperature (black lines) and in the ground state at finite temperature (red thick line).

Here  $\psi_e = (\psi_{e+}, \psi_{e-})^T$  and  $\phi_h = (-\phi_{h-}, \phi_{h+})^T$  are the spinors for electron and hole, respectively. We assume  $\Delta(x) = \Delta_0 \{e^{i\varphi_L} \vartheta(-x) + e^{i\varphi_R} \vartheta(x-L)\}$  with the step function  $\vartheta(t) = 1$  for  $t \geq 0$  and 0 for  $t < 0$ . The phase difference between two superconductors is defined as  $\varphi \equiv \varphi_L - \varphi_R$ . The energy  $E$  is measured from the Fermi level  $E_F$ .  $H$  in the diagonal element is the free-electron Hamiltonian. In our model,  $H = H_0 + H_{SO} + H_Z$  with  $H_0 = p_x^2/(2m^*)$ , the SO interaction  $H_{SO} = \alpha \cdot \hat{\sigma} p_x/\hbar$ , and the Zeeman effect due to an external magnetic field  $H_Z = g\mu_B \mathbf{B} \cdot \hat{\sigma}/2$  using effective mass  $m^*$ ,  $g$ -factor  $g$  ( $\approx -50$  for InSb), Bohr magneton  $\mu_B$ , and Pauli matrices  $\hat{\sigma}$ . The time-reversal operator  $\mathcal{T} = -i\hat{\sigma}_y K$  satisfies  $\mathcal{T}H_{SO}\mathcal{T}^{-1} = H_{SO}$  and  $\mathcal{T}H_Z\mathcal{T}^{-1} = -H_Z$ .  $K$  is the operator to form a complex conjugate;  $Kf = f^*$ . The Hamiltonian is rewritten as

$$H = \frac{p_x^2}{2m^*} - \frac{\alpha}{\hbar} p_x \hat{\sigma}_\theta - \frac{1}{2} E_Z \hat{\sigma}_z \quad (2)$$

by choosing proper axis in spin space. Here  $\hat{\sigma}_\theta = \hat{\sigma}_z \cos \theta + \hat{\sigma}_x \sin \theta$  with  $\theta$  being the angle between the external field and the effective SO field.  $E_Z \equiv |g\mu_B B|$ .

The magnetic field is assumed to be screened in the superconducting region and the Zeeman energy  $E_Z$  is non-zero only at  $0 < x < L$ . For a large  $g$ -factor in InSb, a large Zeeman energy is obtained for weak magnetic field, which does not break the superconductivity. We assume a short junction with  $L \ll \xi \equiv \hbar v_F/(\pi \Delta_0)$ . No potential barrier is assumed at the boundaries between the normal and superconducting regions, so that the electron propagation in the nanowire is completely ballistic.  $E_Z$  and  $\Delta_0$  are much smaller than  $E_F$ .

The BdG equation in Eq. (1) gives a pair of Andreev lev-

els. When the BdG equation has an eigenenergy  $E_n(\varphi)$  with eigenvector  $(\psi_{e,n}, \phi_{h,n})^T$ ,  $-E_n(\varphi)$  is also an eigenenergy of the equation with  $(-\mathcal{T}\phi_{h,n}, \mathcal{T}\psi_{e,n})^T$ .

**CALCULATION AND RESULTS.** – The BdG equation in Eq. (1) can be written in terms of the scattering matrix [22]. We focus on a single conduction channel in the nanowire.

Let us consider the wavefunction of the form  $(\psi_e, \phi_h)^T = e^{\pm i k_F x} (\psi_e^{(\pm)}, \phi_h^{(\pm)})^T$ . The envelope function with positive (negative) sign corresponds to the quasiparticle for right-going (left-going) electron and left-going (right-going) hole. The BdG equation for the envelope function is given by

$$\begin{pmatrix} \mp i \hbar v_F \partial_x - \mathbf{h}_\pm \cdot \hat{\sigma} & \Delta(x) \\ \Delta^*(x) & \pm i \hbar v_F \partial_x - \mathbf{h}_\mp \cdot \hat{\sigma} \end{pmatrix} \begin{pmatrix} \psi_e^{(\pm)} \\ \phi_h^{(\pm)} \end{pmatrix} = E \begin{pmatrix} \psi_e^{(\pm)} \\ \phi_h^{(\pm)} \end{pmatrix} \quad (3)$$

with

$$\mathbf{h}_\pm = \frac{1}{2} E_Z \mathbf{e}_z \pm \alpha k_F \mathbf{e}_\theta, \quad (4)$$

which means a total magnetic field for electron and hole. Here  $\partial_x^2 \psi_e^{(\pm)}$  and  $\alpha(\partial_x \psi_e^{(\pm)})$  terms and those for hole are neglected when  $E_F \gg \Delta_0$ .

The quantum transport of electron (hole) in the normal region ( $\Delta = 0$ ) with SO interaction and Zeeman effect is described by the scattering matrix  $S_e$  ( $S_h$ ). The wavefunctions of electron and hole are  $\psi_e^{(\pm)}(x) \propto \exp(\mp i \frac{E + \mathbf{h}_\pm \cdot \hat{\sigma}}{\hbar v_F} x)$  and  $\phi_h^{(\pm)}(x) \propto \exp(\pm i \frac{E + \mathbf{h}_\mp \cdot \hat{\sigma}}{\hbar v_F} x)$ , respectively. The scattering matrices are related to each other by  $\hat{S}_h(E) = \hat{g} \hat{S}_e^*(-E) \hat{g}^\dagger$  with  $\hat{g} \equiv -i\hat{\sigma}_y$ . On the assumption that they are independent of energy  $E$  for  $|E| < \Delta_0$ , and thus  $\hat{S}_h = \hat{g} \hat{S}_e^* \hat{g}^\dagger$ . The transmission coefficient for the ballistic nanowire is unity. We denote  $\hat{S}_e = \hat{S}$ :

$$\hat{S} = \begin{pmatrix} & \hat{t}_{LR} \\ \hat{t}_{RL} & \end{pmatrix}, \quad (5)$$

where

$$\hat{t}_{RL} = \exp\left(i \frac{L}{\hbar v_F} \mathbf{h}_+ \cdot \hat{\sigma}\right), \quad \hat{t}_{LR} = \exp\left(-i \frac{L}{\hbar v_F} \mathbf{h}_- \cdot \hat{\sigma}\right) \quad (6)$$

mean dynamical phases for spins by SO interaction and Zeeman effect (see supplementary note).

The Andreev reflection at  $x = 0$  and  $L$  is also described in terms of scattering matrix  $\hat{r}_{he}$  for the conversion from electron to hole and  $\hat{r}_{eh}$  for that from hole to electron [22]:

$$\hat{r}_{he} = e^{-i\alpha_A} \begin{pmatrix} e^{-i\varphi_L} & \\ & e^{-i\varphi_R} \end{pmatrix}, \quad \hat{r}_{eh} = e^{-i\alpha_A} \begin{pmatrix} e^{i\varphi_L} & \\ & e^{i\varphi_R} \end{pmatrix} \quad (7)$$

with  $\alpha_A \equiv \arccos(E/\Delta_0)$ . It is important that  $\hat{r}_{he(eh)}$  does not depend on SO interaction.

The product of scattering matrices gives an equation,  $\det(\hat{1} - \hat{r}_{eh}(\hat{g} \hat{S}^* \hat{g}^\dagger) \hat{r}_{he} \hat{S}) = 0$ , which is equivalent with the BdG equation in Eq. (1), and gives the energies of Andreev levels. By substituting Eqs. (5) and (7), we obtain

$$\det(\hat{1} - e^{-i(2\alpha_A - \varphi)} \hat{t}_{LR} \hat{t}_{RL}) = 0, \quad (8)$$

$$\det(\hat{1} - e^{-i(2\alpha_A + \varphi)} \hat{t}_{RL} \hat{t}_{LR}) = 0. \quad (9)$$

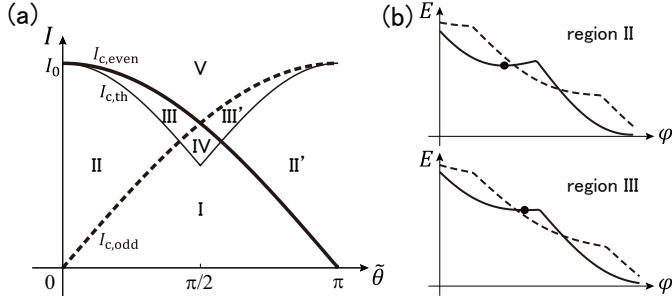


Fig. 2: (a) Critical current as a function of the phase  $\tilde{\theta}$ . Solid and broken lines indicate the current for the even and odd parity states, respectively, whereas thin line is one for the “thermodynamic” current. (b) Schematic view of energy at a finite current bias as a function of  $\varphi$ . Solid and broken lines corresponds to the even and odd parities, respectively. The dot indicates a stable point for even parity. In the regions II and III, stable point is absent for odd parity.

Eq. (8) corresponds to the Andreev bound states with clockwise path (right-going electron and left-going hole) schematically shown in Fig. 1(b), whereas Eq. (9) is a counterclockwise path. The energies of Andreev level are given by

$$E_{\cup,\pm}(\varphi) = \Delta_0 \cos\left(\frac{\varphi \pm \tilde{\theta}}{2}\right), \quad (10)$$

$$E_{\cup,\pm}(\varphi) = \Delta_0 \cos\left(\frac{-\varphi \pm \tilde{\theta} + 2\pi}{2}\right) = -E_{\cup,\mp}(\varphi) \quad (11)$$

for clockwise and counterclockwise paths, respectively. The phase  $\tilde{\theta} \in [0, \pi]$  is defined as

$$\cos \tilde{\theta} \equiv \cos \theta_+ \cos \theta_- - (\mathbf{n}_+ \cdot \mathbf{n}_-) \sin \theta_+ \sin \theta_- \quad (12)$$

with  $\theta_{\pm} = |\mathbf{h}_{\pm}|L/(\hbar v_F)$  [23].  $\mathbf{n}_{\pm} = \mathbf{h}_{\pm}/|\mathbf{h}_{\pm}|$  are unit vectors. We introduce parameters  $\theta_B \equiv E_Z L/(\hbar v_F)$  and  $\theta_{SO} \equiv 2\alpha k_F L/(\hbar v_F)$  for the magnetic field and SO interaction, respectively.

The ground state energy is given by  $E_{gs}(\varphi) = (1/2)\sum_n' E_n(\varphi)$  where the summation is taken over all with negative energy levels. The ground state is spin singlet in the absence of magnetic field. In excited states, positive levels are populated [24]. When the magnetic field is weak,  $E_{\cup,\pm}$  and  $E_{\cup,\pm}$  are positive and negative at  $\varphi = 0$ , respectively. We plot schematically the energies of junction with zero [ $E_0(\varphi) = (E_{\cup,+} + E_{\cup,-})/2$ ], one [ $E_{1\pm}(\varphi) = E_0 + E_{\cup,\pm}$ ], and two quasiparticles [ $E_2(\varphi) = E_0 + (E_{\cup,+} + E_{\cup,-})$ ] in Fig. 1(c). The fermion parity of  $E_0$  and  $E_2$  is even, whereas  $E_{1\pm}$  is odd. At zero temperature, the parity is conserved and  $E_{1\pm}$  states can not relax to  $E_0$  or  $E_2$  [24].

The supercurrents via the even and odd states are calculated by the differential of the energies at  $\varphi$ ,  $I_p(\varphi) = (e/\hbar)dE_p(\varphi)/d\varphi$  ( $p = \text{even or odd}$ ), where  $E_{\text{even}} = \min(E_0, E_2)$  and  $E_{\text{odd}} = \min(E_{1+}, E_{1-})$ . Figure 1(d) shows schematically the supercurrent

$$I_{\text{even}}(\varphi) = \begin{cases} I_0 \cos(\tilde{\theta}/2) \sin(\varphi/2) & \text{for } 0 \leq \varphi < \pi \\ -I_0 \cos(\tilde{\theta}/2) \sin(\varphi/2) & \text{for } \pi \leq \varphi < 2\pi \end{cases} \quad (13)$$

$$I_{\text{odd}}(\varphi) = -I_0 \sin(\tilde{\theta}/2) \cos(\varphi/2) \quad (14)$$

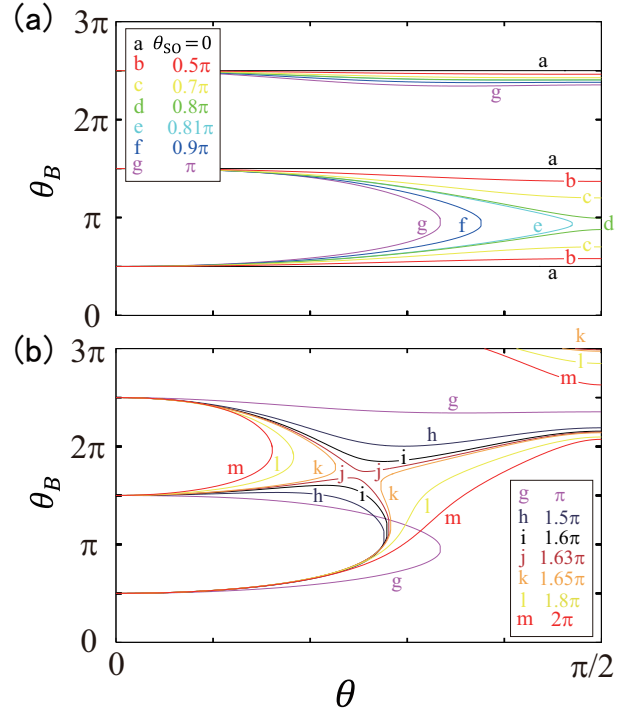


Fig. 3: Position of cusps of critical current in the plane of angle  $\theta$  and magnetic field  $\theta_B = E_Z L/(\hbar v_F)$ . The SO interaction increases from  $\theta_{SO} = 0$  to  $\pi$  (a) and  $\pi$  to  $2\pi$  (b) with  $\theta_{SO} = 2\alpha k_F L/(\hbar v_F)$ .

with  $I_0 \equiv e\Delta_0/\hbar$ . In the presence of magnetic field, the energy of odd parity,  $E_{1+}$ , is lower than the even parity,  $E_0$  and  $E_2$  at  $|\varphi - \pi| < \tilde{\theta}$ . At finite temperature, the parity can change since the quasiparticle can enter or leave the junction. If the parity switches immediately, the “thermodynamic” current  $I_{th}(\varphi)$  of is determined from  $E_{gs}$ ,

$$I_{th}(\varphi) = \begin{cases} I_0 \cos(\tilde{\theta}/2) \sin(\varphi/2) & \text{for } 0 \leq \varphi < \pi - \tilde{\theta} \\ -I_0 \sin(\tilde{\theta}/2) \cos(\varphi/2) & \text{for } \pi - \tilde{\theta} \leq \varphi < \pi + \tilde{\theta} \\ -I_0 \cos(\tilde{\theta}/2) \sin(\varphi/2) & \text{for } \pi + \tilde{\theta} \leq \varphi < 2\pi \end{cases} \quad (15)$$

The critical currents for even and odd parities and thermodynamic one are

$$I_{c,\text{even}} = I_0 \cos(\tilde{\theta}/2) \quad (16)$$

$$I_{c,\text{odd}} = I_0 \sin(\tilde{\theta}/2), \quad (17)$$

$$I_{c,\text{th}} = \begin{cases} I_0 \cos^2(\tilde{\theta}/2) & \text{for } \tilde{\theta} < \pi/2 \\ I_0 \sin^2(\tilde{\theta}/2) & \text{for } \tilde{\theta} \geq \pi/2 \end{cases}, \quad (18)$$

respectively. At zero temperature, the critical current should be  $\max(I_{c,\text{even}}, I_{c,\text{odd}})$ , which is larger than  $I_{c,\text{th}}$  [Fig. 2(a)]. In Fig. 2(a), we divide the  $I$ - $\tilde{\theta}$  plane into five regions. For an applied current  $I$  which satisfies  $I_{c,\text{even}} > I > I_{c,\text{odd}}$ , the currents via the even and odd parity state accompany no and finite voltage, respectively. The dynamics of phase difference  $\varphi$  in the junction at a finite current is intuitively understood by the so-called tilted washboard model [25]. The energy for even and odd parities at the current  $I$  is given as  $E_p(\varphi, I) = E_p(\varphi) - (\hbar I/2e)\varphi$ . If  $E_p(\varphi, I)$  has a stable point, where  $\partial E_p/\partial \varphi = 0$ , the current accompanies

zero voltage [Fig. 2(b)]. At finite low temperature, the parity is switched by the thermal fluctuation. In experiments, the time average of voltage should indicate a small value, which is determined by the ration between the dwell time in odd and even states,  $\tau_o/\tau_e$ . In region II in Fig. 2(a),  $\tau_o/\tau_e \ll 1$  since the stable point of even parity state is energetically lower than the energy of odd one at the same phase difference  $\varphi$  [upper panel in Fig. 2(b)]. In region III, the stable point of even parity is not energetically favorable (lower panel) and  $\tau_o/\tau_e$  is larger. The regions are distinguished by the voltage measurement and its temperature dependence.

The critical current is determined by the phase  $\tilde{\theta}$  and the position of cusp is located at  $\tilde{\theta} = \pi/2$  for both  $\max(I_{c,\text{even}}, I_{c,\text{odd}})$  and  $I_{c,\text{th}}$ . The  $0-\pi$  transition also takes place at  $\tilde{\theta} = \pi/2$ . Therefore we focus on the position of cusp and does not take care about the parity effect on the critical current oscillation. When the external magnetic field is parallel with the effective SO field,  $\cos \tilde{\theta} = \cos \theta_B$  and the cusp positions are periodic in magnetic field corresponding to  $\theta_B = (2n+1)\pi/2$  with an integer  $n$ . The SO interaction modulates the critical current when  $\theta \neq 0$ . Figure 3 shows the position of cusps as the magnetic field is rotated. The distance of the first and the second cusps shortens with increasing of  $\theta_{SO}$ . The disappearance of two cusps (and  $0-\pi$  transition) takes place at  $\theta_{SO} > 0.8\pi$ . If the SO interaction is stronger, the second and the third cusps are closer to each other and vanish. In that case, the first cusp survives for all  $\theta$ .

We plot the critical current  $I_{c,\text{th}}$  at  $\theta = 0.4\pi$  as a function of magnetic field in Fig. 4. The plots show clearly the convergence and annihilation of the first and second cusps with increase of SO interaction. The position of the third cusp also shifts to weaker magnetic field. The critical current at  $\theta_B \approx \pi$  decreases upon increase of  $\theta_{SO}$  since the phase  $\tilde{\theta}$  in this case does not reach  $\pi$ . The disappearance of the cusps is induced by the strong suppression of  $\tilde{\theta}$ . In the absence of SO interaction,  $\mathbf{n}_+ \cdot \mathbf{n}_- = 1$  and Eq. (12) becomes  $\cos \tilde{\theta} = \cos(\theta_+ + \theta_-)$ . In the presence of SO interaction, the total magnetic fields for electron and hole in Eq. (4) are not parallel ( $\mathbf{n}_+ \cdot \mathbf{n}_- < 1$ ), which results in a cancellation of phase by  $\theta_{\pm}$  in Eq. (12). The phase  $\tilde{\theta}$  is generally a nonmonotonic function of  $\theta_B$  and a local minimum of critical current without the cusp is found.

This model can explain the experimental results of differential resistance  $dV/dI$  qualitatively [13]. In the experiment, the positions of local minimum of critical current for parallel and perpendicular magnetic field to the nanowire are different. By tracing the position for all direction of magnetic field, the orientation of effective field can be evaluated.

We have demonstrated a numerical simulation with Rashba SO interaction, the result of which agrees with this simple model [26]. In this model, the anomalous Josephson current,  $I(\varphi = 0) \neq 0$ , is not obtained even in the presence of SO interaction. The anomalous effect is caused by the spin-dependent channel mixing due to the SO interaction in previous studies [18, 19]. If we take into account more than one conduction channel, the anomalous effect is found.

The anisotropy of g-factor in the nanowire also contributes to the anisotropy of critical current oscillation. However, the g-factor anisotropy only shifts the position of cusps and does not

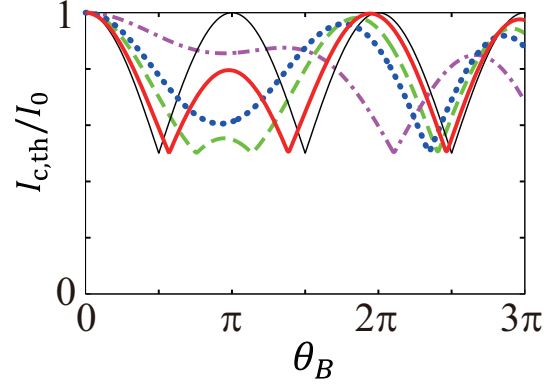


Fig. 4: Critical current  $I_{c,\text{th}}$  as a function of external magnetic field when  $\theta = 0.4\pi$ . The strength of SO interaction is  $2\alpha k_F L/(\hbar v_F) = 0.5\pi$  (solid),  $0.8\pi$  (broken),  $\pi$  (dotted), and  $1.5\pi$  (dotted broken lines). Thin line corresponds to the absence of SO interaction.  $I_0 \equiv e\Delta_0/\hbar$ .

induce the disappearance of  $0-\pi$  transition. In the experiment for nanowire quantum dots, the g-factor is the largest for a parallel direction to the nanowire [2], which would shorten the oscillation period although the period is the longest for the parallel magnetic field in the experiment. Gharavi *et al.* have examined the critical current oscillation in InAs nanowire, which is attributed not to the Zeeman effect but to the orbital effect [11]. The orbital effect may contribute to the anisotropy.

**CONCLUSIONS.** – In conclusions, we have studied the effect of SO interaction on the critical current in semiconductor nanowire Josephson junction within a minimal model. The critical current oscillates as a function of magnetic field. The effective field due to the SO interaction causes the magnetic anisotropy. We focus on the position of cusps of critical current that signal the  $0-\pi$  transition. The oscillation and its anisotropy are governed by a single phase  $\tilde{\theta}$  that combines the effect of magnetic field and SO interaction. We have also considered the parity effect on the Josephson current at low temperature. Although the parity conservation changes the supercurrent and the character of superconducting transport, it does not affect the positions of the cusps.

\* \* \*

We acknowledge fruitful discussions about experiments with Professor L. P. Kouwenhoven, A. Geresdi, V. Mourik, K. Zuo of Delft University of Technology and about theory with G. Campagnano, P. Lucignano, Professor A. Tagliacozzo of the University of Naples and D. Giuliano of CNR-SPIN. We acknowledge financial support by the Motizuki Fund of Yukawa Memorial Foundation. T.Y. is a JSPS Postdoctoral Fellow for Research Abroad.

## REFERENCES

- [1] NADJ-PERGE S., FROLOV S. M., BAKKERS E. P. A. M. and KOUWENHOVEN L. P., *Nature*, **468** (2010) 1084.



- [2] NADJ-PERGE S., PRIBIAG V. S., VAN DEN BERG J. W. G., ZUO K., PLISSARD S. R., BAKKERS E. P. A. M., FROLOV S. M. and KOUWENHOVEN L. P., *Phys. Rev. Lett.*, **108** (2012) 166801.
- [3] KITAEV A. YU., *Phys.-Usp.*, **44** (2001) 131.
- [4] MOURIK V., ZUO K., FROLOV S. M., PLISSARD S. R., BAKKERS E. P. A. M. and KOUWENHOVEN L. P., *Science*, **336** (2012) 1003.
- [5] DAS A., RONEN Y., MOST Y., OREG Y., HEIBLUM M. and SHTRIKMAN H., *Nature Phys.*, **8** (2012) 887.
- [6] DENG M. T., YU C. L., HUANG G. Y., LARSSON M., CAROFF P. and XU H. Q., *Nano Lett.*, **12** (2012) 6414.
- [7] DOH Y.-J., VAN DAM J. A., ROEST A. L., BAKKERS E. P. A. M., KOUWENHOVEN L. P. and DE FRANCESCHI S., *Science*, **309** (2005) 272.
- [8] VAN DAM J. A., NAZAROV YU. V., BAKKERS E. P. A. M., DE FRANCESCHI S. and KOUWENHOVEN L. P., *Nature*, **442** (2006) 667.
- [9] NILSSON H. A., SAMUELSSON P., CAROFF P. and XU H. Q., *Nano Lett.*, **12** (2011) 228.
- [10] ROKHINSON L. P., LIU X. and FURDYNA J. K., *Nature Phys.*, **8** (2012) 795.
- [11] GHARAVI K., HOLLOWAY G. W., HAAPAMAKI C. M., ANSARI M. H., MUHAMMAD M., LAPIERRE R. R. and BAUGH J., *arXiv*, (2014) cond-mat/1405.7455.
- [12] LI C., KASUMOV A., MURANI A., SENGUPTA S., FORTUNA F., NAPOLSKII K., KOSHKODAEV D., TSIRLINA G., KASUMOV Y., KHODOS I., DEBLOCK R., FERRIER M., GUÉRON S. and BOUCHIAT H., *arXiv*, (2014) cond-mat/1406.4280.
- [13] KOUWENHOVEN L. P., FROLOV S. M., GERESDI A., MOURIK V. and ZUO K., , (2014) private communications.
- [14] OBOZNOV V. A., BOL'GINOV V. V., FEOFANOV A. K., RYAZANOV V. V. and BUZDIN A. I., *Phys. Rev. Lett.*, **96** (2006) 197003.
- [15] FU L. and KANE C. L., *Phys. Rev. B*, **79** (2009) 161408(R).
- [16] BEENAKKER C. W. J., PIKULIN D. I., HYART T., SCHOMERUS H. and DAHLHAUS J. P., *Phys. Rev. Lett.*, **110** (2013) 017003.
- [17] BUZDIN A., *Phys. Rev. Lett.*, **101** (2008) 107005.
- [18] YOKOYAMA T., ETO M. and NAZAROV YU. V., *J. Phys. Soc. Jpn.*, **82** (2013) 054703.
- [19] YOKOYAMA T., ETO M. and NAZAROV YU. V., *Phys. Rev. B*, **89** (2014) 195407.
- [20] TAKAHASHI S., DEACON R. S., YOSHIDA K., OIWA A., SHIBATA K., HIRAKAWA K., TOKURA Y. and TARUCHA S., *Phys. Rev. Lett.*, **104** (2010) 246801.
- [21] NAZAROV YU. V. and BLANTER Y. M., *Quantum Transport: introduction to nanoscience* (Cambridge University Press, Cambridge) 2009.
- [22] BEENAKKER C. W. J., *Phys. Rev. Lett.*, **67** (1991) 3836; *Phys. Rev. Lett.*, **68** (1992) 1442(E).
- [23] We use a mathematical formula for the Pauli matrix,  $e^{ian_a\hat{\sigma}}e^{ibn_b\hat{\sigma}} = e^{icn_c\hat{\sigma}}$ , where  $\cos c = \cos a \cos b - (\mathbf{n}_a \cdot \mathbf{n}_b) \sin a \sin b$  and  $\mathbf{n}_c \sin c = \{\mathbf{n}_a \sin a \cos b + \mathbf{n}_b \cos a \sin b - (\mathbf{n}_a \times \mathbf{n}_b) \sin a \sin b\}$ .
- [24] CHITCHELKATCHEV N. M. and NAZAROV YU. V., *Phys. Rev. Lett.*, **90** (2003) 226806.
- [25] TINKHAM M., *Introduction to superconductivity second edition* (DOVER PUBLICATION INC., New York) 2004.
- [26] YOKOYAMA T., ETO M. and NAZAROV YU. V., *arXiv*, (2014) cond-mat/1408.0194.

## Supplementary note. —

In this supplementary note, we introduce a detail calculation of scattering-matrix approach in our minimal model. We also explain the parity switching on the tilted washboard model and some additional results to support an understanding of physics.

**Scattering-matrix in the normal region.** — The BdG equation for the envelope function is given by Eq. (3) in the main text:

$$\begin{pmatrix} \mp i\hbar v_F \partial_x - \mathbf{h}_\pm \cdot \hat{\sigma} & \Delta(x) \\ \Delta^*(x) & \pm i\hbar v_F \partial_x - \mathbf{h}_\mp \cdot \hat{\sigma} \end{pmatrix} \begin{pmatrix} \psi_e^{(\pm)} \\ \phi_h^{(\pm)} \end{pmatrix} = E \begin{pmatrix} \psi_e^{(\pm)} \\ \phi_h^{(\pm)} \end{pmatrix} \quad (19)$$

with

$$\mathbf{h}_\pm = \frac{1}{2} E_Z \mathbf{e}_z \pm \alpha k_F \mathbf{e}_\theta, \quad (20)$$

which means a total magnetic field for electron and hole. Let us concentrate on the right-going electron  $\psi_e^{(+)}(x)$  in the normal region ( $\Delta = 0$ ). The transmission matrix  $\hat{t}_{\text{RL}}$  connects the wavefunctions at  $x = 0$  and  $L$ ,

$$\begin{pmatrix} \psi_{e+}^{(+)}(L) \\ \psi_{e-}^{(+)}(L) \end{pmatrix} = \hat{t}_{\text{RL}} \begin{pmatrix} \psi_{e+}^{(+)}(0) \\ \psi_{e-}^{(+)}(0) \end{pmatrix}. \quad (21)$$

The wavefunction  $\psi_e^{(+)}(x)$  obeys a following equation,

$$\partial_x \psi_e^{(+)} = +i \frac{E + \mathbf{h}_+ \cdot \hat{\sigma}}{\hbar v_F} \psi_e^{(+)} \equiv \hat{f}^{(+)} \psi_e^{(+)}. \quad (22)$$

$\hat{f}^{(+)}$  is a  $2 \times 2$  matrix in the spin space. We diagonalize this matrix by an unitary matrix,  $\hat{U}^\dagger \hat{f}^{(+)} \hat{U} = \text{diag}(\lambda_+, \lambda_-)$ . If we define as  $\xi_e^{(+)} = \hat{U}^\dagger \psi_e^{(+)}$ , Eq. (22) is rewritten as

$$\partial_x \begin{pmatrix} \xi_{e+}^{(+)}(x) \\ \xi_{e-}^{(+)}(x) \end{pmatrix} = \begin{pmatrix} \lambda_+ & \\ & \lambda_- \end{pmatrix} \begin{pmatrix} \xi_{e+}^{(+)}(x) \\ \xi_{e-}^{(+)}(x) \end{pmatrix}. \quad (23)$$

The solution of this equation,  $\xi_{e\pm}^{(+)}(x) \propto e^{\lambda_\pm x}$ , results in

$$\psi_e^{(+)}(L) = \hat{U} \begin{pmatrix} e^{\lambda_+ L} & \\ & e^{\lambda_- L} \end{pmatrix} \hat{U}^\dagger \psi_e^{(+)}(0). \quad (24)$$

By comparing Eq. (21) and (24), we obtain the transmission matrix  $\hat{t}_{\text{RL}}$  in Eq. (6) in the main text,

$$\hat{t}_{\text{RL}} = \exp \left( i \frac{L}{\hbar v_F} \mathbf{h}_+ \cdot \hat{\sigma} \right), \quad (25)$$

where the energy dependent term is neglected. The transmission matrix for left-going electron,  $\hat{t}_{\text{LR}}$ , is calculated in the same way. The scattering-matrix for hole is also obtained directly from the equation of  $\phi_h^{(\pm)}$ , which satisfies the relation  $\hat{S}_h = \hat{g} \hat{S}_e^* \hat{g}^\dagger$ .

### Andreev reflection with spin-orbit interaction. —

The Andreev reflection is also expressed in terms of scattering-matrix, the expression of which is developed by Beenakker [22]. Beenakker formulates  $\hat{r}_{\text{he}}$  and  $\hat{r}_{\text{eh}}$  in the absence of SO interaction. We consider the Andreev reflection with SO interaction and show that the SO interaction does not affect the Andreev reflection coefficient.

We assume SN interface at  $x = 0$ . The superconducting and normal regions are  $x > 0$  and  $x < 0$ , respectively. No magnetic field is applied. For  $|E| < \Delta_0$  in the superconducting region, the envelope function of  $\Psi(x) = e^{+ik_F x} \tilde{\Psi}(x)$  decays exponentially,  $\tilde{\Psi}(x) = (f_e, f_h)^T \exp[-\kappa x / \hbar v_F]$ . By substituting  $\tilde{\Psi}(x)$  into the BdG equation,

$$\begin{pmatrix} +ik - \mathbf{h}_{\text{SO}} \cdot \hat{\sigma} - E & \Delta \\ \Delta^* & -ik + \mathbf{h}_{\text{SO}} \cdot \hat{\sigma} - E \end{pmatrix} \begin{pmatrix} f_e \\ f_h \end{pmatrix} = 0. \quad (26)$$

The solution is  $\kappa = -\sqrt{\Delta_0^2 - E^2} \pm i|\mathbf{h}_{\text{SO}}|$ . Thus the SO interaction induces the oscillation component in the evanescent wave. The spin quantization axis is taken in the direction of  $\mathbf{h}_{\text{SO}}$ . The Andreev reflection coefficient converting electron to hole is given as

$$f_h/f_e = \frac{\Delta^*}{E + i\sqrt{\Delta_0^2 - E^2}} = \exp \left( -\varphi - \arccos \frac{E}{\Delta_0} \right), \quad (27)$$

which is the same result as that without SO interaction.

**Parity switching.** — At zero temperature, the quasiparticle fermion parity is conserved. Thus the junction energy or supercurrent for even and odd parity are taken into account. The junction energies with zero, one, and two quasiparticles are given in the main text as

$$E_0(\varphi) = -\Delta_0 \cos(\tilde{\theta}/2) \cos(\varphi/2), \quad (28)$$

$$E_{1\pm}(\varphi) = \mp \Delta_0 \sin(\tilde{\theta}/2) \sin(\varphi/2), \quad (29)$$

$$E_2(\varphi) = \Delta_0 \cos(\tilde{\theta}/2) \cos(\varphi/2), \quad (30)$$

respectively. Two quasiparticles can enter into or leave from the junction immediately if the parity does not change. The energies for even and odd parity are  $E_{\text{even}}(\varphi) = \min(E_0, E_2)$  and  $E_{\text{odd}}(\varphi) = \min(E_{1+}, E_{1-})$ , respectively. The supercurrents via even and odd parity state in Eqs. (13) and (14) in the main text are calculated by the differential of the energies at  $\varphi$ ,  $I_p(\varphi) = (e/\hbar) dE_p(\varphi)/d\varphi$  ( $p = \text{even or odd}$ ). When the temperature is enough high, the parity changes immediately. In this case, the energy of junction is given by the ground state energy  $E_{\text{gs}}(\varphi) = \min(E_0, E_{1\pm}, E_2)$  and the current becomes  $I_{\text{th}}(\varphi)$  in Eq. (15) in the main text.

When a bias voltage is applied to the junction, the phase difference  $\varphi$  would evolve according to  $d\varphi/dt = 2eV/\hbar$ . In other word,  $\varphi$  would be fixed if the voltage is zero and only the supercurrent flows. The dynamics of phase difference is understood intuitively by the so-called tilted washboard model [25]. The energy for even and odd parities at the current  $I$  is given as

$$E_p(\varphi, I) = E_p(\varphi) - (\hbar I / 2e) \varphi. \quad (31)$$

The phase difference  $\varphi$  runs down on this potential. If  $E_p(\varphi, I)$  has a stable point, which means  $\partial E_p / \partial \varphi = 0$ ,  $\varphi$  stops at the stable point and the current flows accompanying zero voltage. When an applied current  $I$  is small, both even and odd parity states have the stable point. As the current increases at  $\tilde{\theta} < \pi/2$ , the stable point for odd parity vanishes, whereas the even one

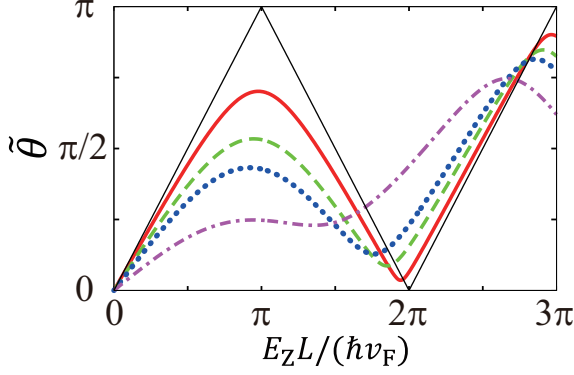


Fig. 5: Phase  $\tilde{\theta}$  as a function of external magnetic field when  $\theta = 0.4\pi$ . The strength of SO interaction is  $2\alpha k_F L / (\hbar v_F) = 0.5\pi$  (solid),  $0.8\pi$  (broken),  $\pi$  (dotted), and  $1.5\pi$  (dotted broken lines). Thin line corresponds to the absence of SO interaction.

has, as shown in Fig. 2(b) in the main text. Then, the current satisfies  $I_{c,\text{even}} > I > I_{c,\text{odd}}$ . Since the fermion parity is kept at zero temperature, the supercurrent is assured by the even parity state.

At finite temperature, the fermion parity can be switched by the thermal fluctuation, which changes the number of quasiparticles in the junction. The probability of parity switching is estimated as  $\sim \exp[-\Delta E(\varphi, I)/(k_B T)]$  with the energy difference  $\Delta E$  between even and odd parity states at phase difference  $\varphi$ . If a stationary current within  $I_{c,\text{even}} > I > I_{c,\text{odd}}$  is applied [region II or III in Fig. 2(a) in the main text], a finite voltage,  $V_o$ , due to the odd parity would be detected by the parity switching. ( $V_e = 0$  in this case.) The time average of measured value of voltage is  $\bar{V} = V_o \tau_o / (\tau_o + \tau_e)$  with  $\tau_{o(e)}$  being the dwell time in odd (even) parity state. The measurement value would be determined by a ration of dwell times  $\tau_o / \tau_e$ . In region II, the current is mainly carried via the even parity state accompanying no voltage, then the phase difference is fixed at the stable point. When the parity switches to odd by the thermal fluctuation, the phase difference goes down on the slope [Fig. 2(b) in the main text]. The energies for the even and odd parity states crosses with each other. The parity can change to the state with lower energy.  $\varphi$  stops at the stable point after the parity is back to even. In region II, the even state energy at the stable point is lower than the energy of odd one at the same phase difference. Thus,  $\varphi$  goes easily back to the stable point, and the dwell time in the odd parity state is much shorter than that in the even one,  $\tau_o \ll \tau_e$ . In region III, on the other hand, the stable point is not favorable energetically, which results a long dwell time in the odd parity. If the parity switching takes place immediately at high temperature,  $\varphi$  relaxes to the lower energy before running on the slope, whereas  $\varphi$  can not stop in region III. Thus, the current accompanies no (finite) voltage in region II (III).

**Additional results for magnetic anisotropy.** – In the main text, we discuss the magnetic anisotropy of critical current and 0- $\pi$  transition. Figure 4 in the main text demonstrates the critical current oscillation  $I_{c,\text{th}}[\tilde{\theta}(\theta_B, \theta_{\text{SO}}, \theta)]$  as the magnetic

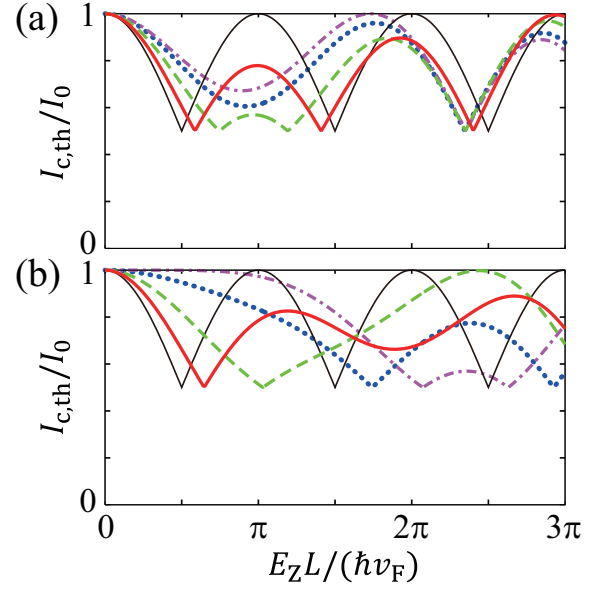


Fig. 6: Critical current  $I_{c,\text{th}}$  as a function of external magnetic field when the magnetic field is rotated. The strength of SO interaction is  $2\alpha k_F L / (\hbar v_F) = \pi$  (a) and  $2\pi$  (b). Solid, broken, dotted, and dotted broken lines correspond to  $\theta = 0.2\pi, 0.3\pi, 0.4\pi$ , and  $0.5\pi$ , respectively. Thin line is  $\theta = 0$ , where the SO interaction does not affect the critical current.  $I_0 \equiv e\Delta_0/\hbar$ .

field is applied at  $\theta = 0.4\pi$  and the SO interaction is gradually increased. Here we show additional results to support an understanding of physics. Figure 5 shows the phase  $\tilde{\theta}$  as a function of magnetic field, where the parameters are the same as those in Fig. 4 in the main text. In the absence of SO interaction, Eq. (12) in the main text becomes  $\cos \tilde{\theta} = \cos \theta_B$ .  $\tilde{\theta} (\in [0, \pi])$  is a sawtooth periodic function of  $\theta_B$  and touches  $\pi$  at  $\theta_B = (2n+1)\pi$  with integer  $n$ . When  $\tilde{\theta} = \pi/2$ , the 0- $\pi$  transition takes place. In the presence of SO interaction,  $\tilde{\theta}$  is deviated from the sawtooth behavior and does not reach  $\pi$ , which corresponds to the suppression of critical current  $I_{c,\text{th}}$ . As  $\theta_{\text{SO}}$  increases, the phase  $\tilde{\theta}$  is suppressed less than  $\pi/2$ , which results in the disappearance of 0- $\pi$  transition around  $\theta_B = \pi$ .

We plot the critical current oscillation additionally when the SO interaction is fixed and the angle  $\theta$  between magnetic field and effective SO field is tuned in Fig. 6. The critical current around  $\theta_B = \pi$  decreases with an increase of angle  $\theta$ . The position of cusps are also modified by the direction of magnetic field. When  $\theta_{\text{SO}} = \pi$ , the first and second cusps are closer to each other with an increase of  $\theta$ , and vanishes. This behavior is similar with that in Fig. 4 in the main text. When  $\theta_{\text{SO}} = 2\pi$ , the first cusp shifts to large  $\theta_B$  by the angle  $\theta$ . These results indicate the magnetic anisotropy of critical current clearly. The periodicity of critical current gives an information of direction of effective SO field.